Derivation and application of blending constraints in lamination parameter space for composite optimisation

Macquart, TBMJ; Bordogna, MT; Lancelot, PMGJ; de Breuker, R

DOI
10.1016/j.compstruct.2015.09.016

Publication date
2016

Document Version
Accepted author manuscript

Published in
Composite Structures

Derivation and Application of Blending Constraints in Lamination Parameter Space for Composite Optimisation

Terence Macquart[1*], Marco T. Bordogna[2] and Paul Lancelot[1],

[1]Faculty of Aerospace Engineering
Delft University of Technology
2629 HS Delft, The Netherlands

[2] DADS - Aéroélasticité et Dynamique des Structures
ONERA
Châtillon, France

Abstract

The present paper proposes a set of blending constraints expressed in lamination parameter space, applicable during the continuous optimisation of composite structures. Thicknesses and ply orientations of large composite structures are often locally optimised in response to unequal spatial load distribution. During this process, ensuring structural continuity is essential in order to achieve designs ready to be manufactured. Single step stacking sequence optimisations relying on evolutionary algorithms to enforce continuity, through the application of blending rules, are prone to the curse of dimensionality. By contrast, multi-step optimisation strategies including a continuous sub-step can optimise composite structures with reasonable computational effort. However, the discrepancies between continuous and discrete optimisation step result in performance loss during stacking sequence retrieval. By deriving and applying blending constraints during the continuous optimisation, this paper aim is to reduce the performance loss observed between optimisation levels. The first part of this paper is dedicated to the derivation of blending constraints. The proposed constraints are then successfully applied to a benchmark blending problem in the second part of this paper. Numerical results demonstrate the achievement of near-optimal easy-to-blend continuous designs in a matter of seconds.

Keywords: Composite materials, Blending, Lamination parameters, Optimisation, Variable Stiffness

I. Introduction

The significant weight saving potential achievable with tailored composite structure is now well-recognised amidst the scientific community. The incentive to manufacture strong yet lightweight structures is also resulting in the increasing use of composite materials in many engineering applications. Moving from metals to composite structures has, however, brought forward a considerable new set of challenges including new failure mechanisms, added complexity and the increased number of design variables. These have led to the development of a broad range of composite design guidelines and optimisation methods [1, 2].

Over the last decade, it has become evident that optimising composite structures raises several difficulties. Amongst these, the non-convex fibre angle design space, mixed-integer design variables and, manufacturability constraints have been recognised as major obstacles [3, 4]. In this paper the authors focus on one of the manufacturing constraints, namely the blending constraint. First

[*] Corresponding author. Email address: T.B.M.J.Macquart@tudelft.nl (T. Macquart) , Tel.: +31619918984

introduced by Kristindottir et al.[5], blending is essential to ensure structural continuity and avoid stress concentration during the design of large composite structures, where thicknesses and ply orientations are often locally optimised. Single and multi-step optimisation strategies have been proposed to solve the complex problems of composite structure optimisation. Single optimisation methods such as guide-based designs [6] and stacking sequence tables [4] are strictly limited to the generation of designs satisfying blending constraints. Although successful on small scale problems, these approaches result in highly constrained optimisation with prohibitively high computational cost. On the other hand, multi-step optimisation strategies divide the optimisation of composite structures into faster and simpler-to solve sub-optimisation problems [7, 8]. Commonly used are bi-step optimisation strategies which separate the continuous and discrete optimisations [9, 10]. Employing intermediate design variables (e.g. lamination parameters), the optimisation is reformulated into a continuous convex optimisation for which fast convergence towards a global optimum is guaranteed [11]. Following the continuous optimisation, a highly constrained discrete optimisation is usually employed to retrieve ready-to-manufacture stacking sequences closely matching the continuous optimisation output results.

Optimal designs obtained after the continuous optimisation generally show the significant improvements achieved by composite structures upon metal-based designs [8]. Nevertheless, retrieving a feasible and manufacture-ready stacking sequence closely matching the continuous results often turns out to be challenging, if not impossible [12]. That is, the manufacture of large composite structure is subject to numerous constraints that are not readily applicable at the continuous optimisation step. Constraints are most often integrated into evolutionary algorithms (i.e. the discrete optimisation) in which they can be easily handled. However, running a lightly constrained continuous optimisation followed by a highly constrained discrete search can result in high disparities between the two optimisation steps. The likelihood of an equivalent of the optimal continuous design existing in the highly constrained design space is therefore not guaranteed. As a consequence, this design spaces disparity will often result in performance loss of the optimised structure during stacking sequence retrieval. In view of the above, the aim of the present paper is to derive a set of continuous blending constraints in order to achieve more realistic continuous design, and therefore reduce the loss of performance observed during stacking sequence retrieval.

The rest of this paper is structured as follows. Section II serves as a brief literature review on blending rules. The derivation of blending constraints in lamination parameter space is addressed in Section III. The proposed constraints are applied to a benchmark optimisation problem in Section IV while the output of this investigation are summarised in Section V.

II. Blending Rules

Various blending definitions have been proposed over the last decade. In his work, Adams et al.[6] consider only inner or outer blending, where the innermost or outermost plies are dropped as shown in Figure 1.a. Van Campen et al.[13] introduce two alternative blending definitions, namely the generalised and relaxed generalised blending as illustrated in Figure 1.b. In the former, two adjacent laminates are blended if all the plies of the thinnest panel are also present in the other panels. The relaxed generalised blending consider two laminates blended if there are no discontinuous plies in physical contact. In the present study, the generalised blending definition of Van Campen et al.[13] is followed.

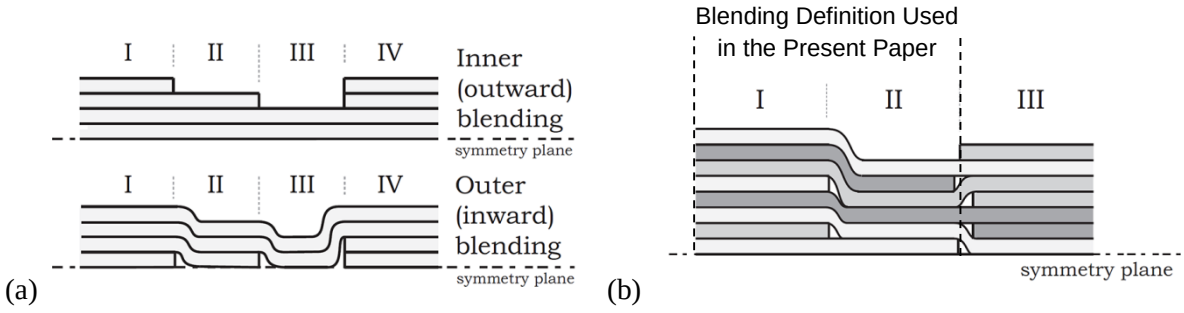

Figure 1 - (a) Outward and inward blending, and (b) generalised (I and II) and relaxed generalised (II and III) blending. Original figures from [13].

The first application of blending in composite optimisation has been performed by Kristinsdottir et al.[5]. Starting from a set of well-defined in-plane loads, the most loaded panel is identified as the thickest laminate. Laminates from other panels are then obtained by progressively dropping plies from this thickest laminate. This "less-then-or-equal-to" blending rule results in a highly constrained global optimisation problem with mixed-integer variables for which Kristinsdottir et al.[5] proposed an improved hit-and-run optimisation strategy. In another investigation, Liu and Haftka [14] used a constrained bi-level optimisation to enforce continuity. Employing a limited number of ply angles, they proposed a continuity constraint expressed as the ratio of common ply angles between adjacent panels. Soremekun et al.[15] proposed a methodology based on a two-step genetic algorithm (GA). In the first step, an optimisation without blending is run to determine the minimum number of plies required in each panel. The second optimisation uses the lowest number plies found in step 1 to create a base laminate spanning the entire structure. The process is then repeated for other group of panels with common number of plies until the final design is reached. Adams et al.[6] introduced yet another blending approach, namely the guide-based blending. Similarly to the "less-then-or-equal-to" blending rule, a guiding stack is defined for the thickest laminate from which other panel laminates are obtained by dropping plies. On the other hand, the guide-based approach reformulates the optimisation problem so as to remove explicit constraints by adding a small number of design variables in order to ensure blending. Adams et al.[6] proposed using a single-step GA to solve the optimisation problem. All of the above mentioned optimisation enforce blending during discrete optimisation. To the best of our knowledge, no reported studies have proposed the application of blending constraints in lamination parameter space for continuous composite optimisation.

III. Derivation of Blending Constraints

Blending constraints in lamination parameter (LP) space are derived in this section. The notation used for LP is first introduced before the reader is guided through the derivation of blending constraints for in-plane and out-of-plane LPs. A general blending constraints, valid for any combinations of LPs, is presented at the end of Section III.

The lamination parameters of a N-ply laminate built out of discrete plies of constant thicknesses and ply angles $\theta(z)$ are calculated as follows:

$$\left(V_1^A, V_2^A, V_3^A, V_4^A\right) = \frac{1}{N}\sum_{i=1}^{N}\left[\cos(2\theta_i), \sin(2\theta_i), \cos(4\theta_i), \sin(4\theta_i)\right] \tag{1.a}$$

$$\left(V_1^B, V_2^B, V_3^B, V_4^B\right) = \frac{2}{(N)^2}\sum_{i=1}^{N}\left(Z_i^2 - Z_{i-1}^2\right)\left[\cos(2\theta_i), \sin(2\theta_i), \cos(4\theta_i), \sin(4\theta_i)\right] \tag{1.b}$$

$$\left(V_1^D, V_2^D, V_3^D, V_4^D\right) = \frac{4}{(N)^3}\sum_{i=1}^{N}\left(Z_i^3 - Z_{i-1}^3\right)[\cos(2\theta_i), \sin(2\theta_i), \cos(4\theta_i), \sin(4\theta_i)] \quad (1.c)$$

where,

$$Z_i = -N/2 + i \quad (2)$$

1. Single In-Plane Lamination Parameter Blending Constraint

The key idea behind the derivation of blending constraints in LP space is to quantify the change in LPs due to ply-drops. The ply-drop notation used throughout this section is presented in Figure 2.

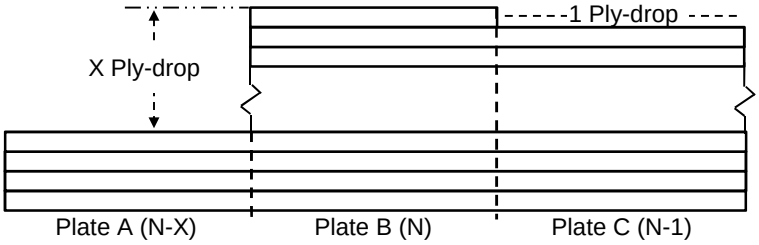

Figure 2 - Ply-drop illustration for N, N-1 and N-X plies

We begin by investigating the difference in the lamination parameter V_1^A due to 1 ply-drop. We denote $V_1^A{}_{(N-1)}$ the value of V_1^A after 1 ply-drop as in (3). The change in V_1^A due to the ply removal can be quantified according to (4), where the subscript *j* refers to the removed ply.

$$V_1^A{}_{(N-1)} = \frac{1}{N-1}\sum_{i=1}^{N-1}\cos(2\theta_i) \quad (3)$$

$$\Delta V_1^A{}_{(N)\to(N-1)} = V_1{}^A{}_{(N)} - V_1{}^A{}_{(N-1)} = \frac{1}{N}\cos(2\theta_j) + \left(\frac{1}{N} - \frac{1}{N-1}\right)\sum_{i=1}^{N-1}\cos(2\theta_i) \quad (4)$$

The maximal and minimal values of (4) respectively occur for [θ_j ; θ_i]= [0° 90°] and for [θ_j ; θ_i]= [90° 0°] at which the magnitude is:

$$\max_{\theta_j,\theta_i}\left\|\Delta V_1^A{}_{(N)\to(N-1)}\right\| = 2/N \quad (5)$$

Equation (5) is verified by generating stacking sequences and computing the change in the lamination parameter V_1^A due to 1 ply-drop. The results are shown in Figure 3 for three pools of stacking sequences: one pool of randomly generated laminates of 20 plies, a second of all symmetric 0/45/90 laminates of 16 plies, and a last pool of extreme laminates of 20 plies. In this context, extreme refers to laminate for which all θ_i are equal to each other. It is important to note that the maximal change in LPs (see Equation (4)) always occurs for an extreme laminate.

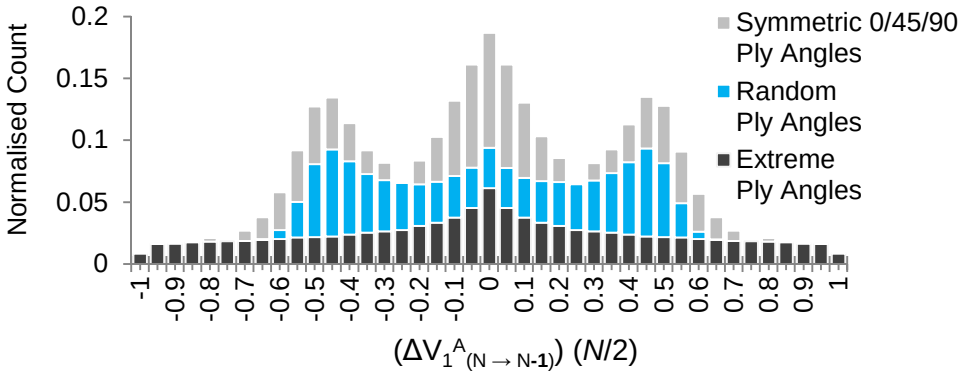

Figure 3 - Normalised change in lamination parameter V_1^A due to 1 ply-drop

Generalising the above results to a random number of X ply-drops we obtain:

$$V_1^A{}_{(N-X)} = \frac{1}{N-X}\sum_{i=X+1}^{N}\cos(2\theta_i) \tag{6}$$

$$\Delta V_1^A{}_{(N)\to(N-X)} = V_1^A{}_{(N)} - V_1^A{}_{(N-X)} = \frac{1}{N}\sum_{j=1}^{X}\cos(2\theta_j) + \left(\frac{1}{N} - \frac{1}{N-X}\right)\sum_{i=X+1}^{N}\cos(2\theta_i) \tag{7}$$

Equation (7) reaches its maximal value for the same configuration as $\Delta V_1^A{}_{(N)\to(N-1)}$ at which the maximal change in the lamination parameter due to X ply-drops is proportional to the ply-drop ratio (X/N):

$$\max_{\theta_j,\theta_i}\left\|\Delta V_1^A{}_{(N)\to(N-X)}\right\| = 2(X/N) \tag{8}$$

Carrying out the equivalent calculations for the remaining in-plane LPs (i.e. $V_{2,3,4}^A$) it can be shown that:

$$\max_{\theta_j,\theta_i}\left\|\Delta V_2^A{}_{(N)\to(N-X)}\right\| = \max_{\theta_j,\theta_i}\left\|\Delta V_3^A{}_{(N)\to(N-X)}\right\| = \max_{\theta_j,\theta_i}\left\|\Delta V_4^A{}_{(N)\to(N-X)}\right\| = 2(X/N) \tag{9}$$

According to (9), four individual blending constraints can therefore be set as follows:

$$\boxed{\Delta V_k^A{}_{(N)\to(N-X)} \le 2(X/N)\,, \quad \text{for } k = 1,2,3,4} \tag{10}$$

Constraints (10) define the maximal change in LPs outside which no blended solution can be found. It should, however, be noted that constraints (10) are very conservative since the occurrence of extreme laminates is unlikely.

2. Coupled In-Plane Lamination Parameters Blending Constraints

Results presented in the previous section only consider the variation of one LP. The simultaneous changes in any combination of in-plane LPs due to ply-drops are investigated herein. We start by investigating the simultaneous change in V_1^A and V_2^A by introducing the in-plane Euclidian distance:

$$E^{ip}_{12\,(N)\to(N-X)} = \sqrt{\left(\Delta V_1^A{}_{(N)\to(N-X)}\right)^2 + \left(\Delta V_2^A{}_{(N)\to(N-X)}\right)^2} \tag{11}$$

Similarly to individual LPs, it can be shown that the maximal Euclidean distance of (11) also occurs for an extreme laminate (subscript *Ext*). As a results, one can expand the first term under the square root as follows:

$$\left[\left(\Delta V_1^A{}_{(N)\to(N-X)}\right)_{Ext}\right]^2 = \left(\frac{1}{N}\cos(2\theta_j)\sum_{j=1}^{X}1 + \left(\frac{1}{N}-\frac{1}{N-X}\right)\cos(2\theta_i)\sum_{i=X+1}^{N}1\right)^2 \tag{12}$$

which simplifies to (13) where $[C_1, C_3] = \left[cos(2\theta_j), cos(2\theta_i)\right]$. We introduce the notation $f_k(\theta_j, \theta_i)$ to denote the sum of cosine and sine functions for extreme laminates where the subscript *k* refers to the lamination parameters considered (i.e. 1, 2, 3 or 4).

$$\left[\left(\Delta V_1^A{}_{(N)\to(N-X)}\right)_{Ext}\right]^2 = (X/N)^2(C_1^2 + C_3^2 - 2C_1C_3) = (X/N)^2 f_1(\theta_j, \theta_i) \tag{13}$$

Carrying out the same procedure for the second term, substituting in (11) and setting $[S_1, S_3] = \left[sin(2\theta_j), sin(2\theta_i)\right]$, the Euclidean distance becomes:

$$\left[\left(E_{12}^{ip}{}_{(N)\to(N-X)}\right)_{Ext}\right]^2 = (X/N)^2\left[\underbrace{(C_1^2 + C_3^2 - 2C_1C_3)}_{from\left(\Delta V_1{}^{A-X}\right)^2} + \underbrace{(S_1^2 + S_3^2 - 2S_1S_3)}_{from\left(\Delta V_2{}^{A-X}\right)^2}\right] = (X/N)^2 f_{12}(\theta_j, \theta_i) \tag{14}$$

Maximizing $f_{12}(\theta_j, \theta_i)$, the maximum in-plane Euclidean distance (11) can be shown to be:

$$\max_{\theta_j,\theta_i}\left[\left(E_{12}^{ip}{}_{(N)\to(N-X)}\right)^2\right] = 4\,(X/N)^2 \tag{15}$$

According to the above derivation, the change in the lamination parameters $V_1{}^A$ and $V_2{}^A$ must satisfy constraint (16). The Euclidian distance (11) is associated to the radius of the feasible lamination parameters space reachable due to ply-drops as illustrated in Figure 4 for a 5-ply laminate and 1 ply-drop.

$$\left(\Delta V_1^A{}_{(N)\to(N-X)}\right)^2 + \left(\Delta V_2^A{}_{(N)\to(N-X)}\right)^2 - 4\,(X/N)^2 \le 0 \tag{16}$$

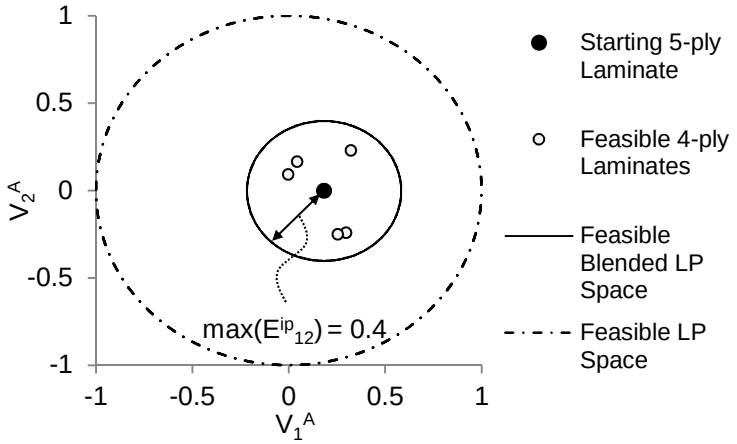

Figure 4 - Illustrative example of the reduced feasible blended lamination parameter space of a stacking sequence of 5 plies due to 1 ply-drop

Generalising the Euclidean distance to all four in plane LPs, one obtains:

$$\left(E^{ip}_{1234_{(N)\to(N-\boldsymbol{X})}}\right)^2 = \sum_{k=1}^{4}\left(\Delta V_k^{A}{}_{(N)\to(N-\boldsymbol{X})}\right)^2 \tag{17}$$

With the following derivation:

$$\left[\left(E^{ip}_{1234_{(N)\to(N-\boldsymbol{X})}}\right)_{Ext}\right]^2 = (X/N)^2[(C_1^2 + C_3^2 - 2C_1C_3) + (S_1^2 + S_3^2 - 2S_1S_3) + (C_2^2 + C_4^2 - 2C_2C_4) + (S_2^2 + S_4^2 - 2S_2S_4)] = (X/N)^2 f_{1234}(\theta_j, \theta_i) \tag{18}$$

In which, the coefficients are given:

$$[C_1, C_2, C_3, C_4\,] = [cos(2\theta_j), cos(4\theta_j), cos(2\theta_i), cos(4\theta_i)] \tag{19}$$

$$[S_1, S_2, S_3, S_4\,] = [sin(2\theta_j), sin(4\theta_j), sin(2\theta_i), sin(4\theta_i)] \tag{20}$$

As previously, the maximal value of (18) is achieved when maximising $f_k(\theta_j, \theta_i)$. This results can be generalised to any possible combination of in-plane lamination parameters considered when calculating the Euclidean distance. The generalised constraint is:

$$\boxed{\left(E^{ip}_{k\ (N)\to(N-\boldsymbol{X})}\right)^2 \leq (X/N)^2\left(\max_{\theta_j,\theta_i} f_k(\theta_j, \theta_i)\right)} \tag{21}$$

for which the maximal values of $f_k(\theta_j, \theta_i)$ for all the in-plane LPs combinations are given in Table 1 and $f_{1234}(\theta_j, \theta_i)$ is plotted as an example in Figure 5.

Table 1 - Maximal values of $f_k(\theta_j, \theta_i)$ for all combination of in-plane lamination parameters

Values of *k*	Corresponding Combination of Lamination Parameters	$\max_{\theta_j,\theta_i} f_k(\theta_j, \theta_i)$
1 or 2 or 3 or 4 or 12 or 34	V_1 or V_2 or V_3 or V_4 or V_1,V_2 or V_3,V_4	4
13 or 23	V_1,V_3 or V_2,V_3	5.1443
14 or 24 or 123 or 124 or 134 or 234 or 1234	V_1,V_4 or V_2,V_4 or V_1,V_2,V_3 or V_1,V_2,V_4 or V_1,V_3,V_4 or V_2,V_3,V_4 or V_1,V_2, V_3,V_4	6.25

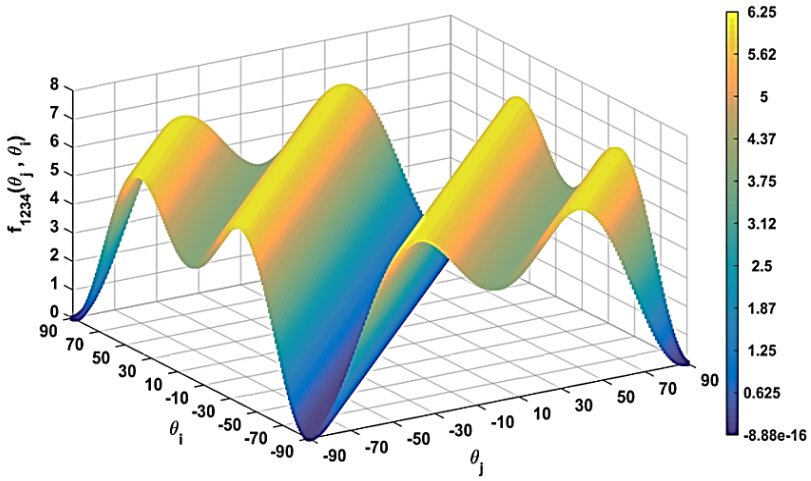

Figure 5 - Coefficient function $f_k(\theta_j, \theta_i)$ for the combination of all in-plane lamination parameters

For sake of clarity, the spherical constraint (21) can be visualised in reduced dimensions when only considering the change of three of the in-plane lamination parameters $\Delta V_k^A{}_{(N)\to(N-X)}$ (k = 1,2,3) as shown in Figure 6.

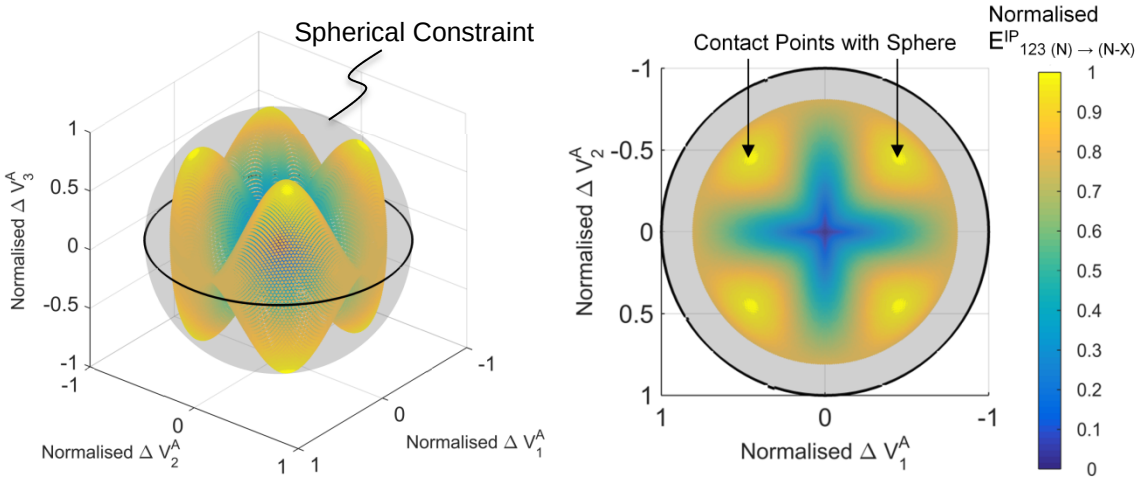

Figure 6 - Normalised Euclidean distance for extreme laminates contained into a sphere of radius 1

Verification

The proposed spherical constraint (21) considering all in-plane lamination parameters is now evaluated. For that purpose, a computer experiment quantifying the ease of a guide-based genetic algorithm in retrieving the stacking sequence of a 2-blended laminates problem is devised. The first laminate is attributed a feasible stacking sequence for which its LPs are calculated. The second laminate LPs are then obtained by disturbing the first laminate LPs with a random vector of variable norm. Next, the GA performance is evaluated while varying the disturbance vector norm so as to obtain LPs inside and outside the spherical constraint derived.

Computer Experiment

(A) Define the initial number of Plies (N), ply-drops (X) and the spherical constraint coefficient (α)

(B) Generate a random stacking sequence of N plies

(C) Calculate the laminate corresponding lamination parameters (LP_N)

(D) Randomly disturb LP_N in order to generate a set of lamination parameter for the second patch LP_{N-X} such that the disturbance satisfies: $\|\Delta LP\| \leq \alpha\left[\sqrt{6.25}(X/N)\right]$.

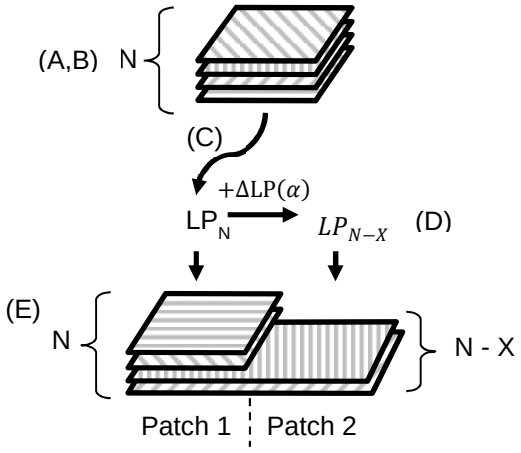

(E) Employ the GA to retrieve a blended stacking sequence matching the LPs. The fitness function is defined is defined as: $Fitness = RMS\left(LP_{obj} - LP_{GA}\right)$
Where $LP_{obj} = [LP_N, LP_{N-X}]$ and $LP_{GA} = [LP_{GA1}, LP_{GA2}]$. LP_{GA1} and LP_{GA2} denotes the LPs retrieved by the GA.

(F) Calculate the GA retrieval error index (E_{index}) defined as the average of the best finesses obtained for each GA runs (i.e. N_{GA}): $E_{index} = \frac{1}{N_{GA}}\sum_{i=1}^{N_{GA}} \min\left(Fitness\ (i)\right)$

Figure 7 - Computer Experiment for verification of the proposed spherical constraint (21)

The computer experiment is run for three examples where the number of plies N is set to 40, the number of repeated GA runs N_{GA} is set to 20, X is respectively (2,4 and 10) and α is variable. The GA attempts to match the continuous LPs by designing blended stacking sequences with ply angles multiples of 15 (i.e. 0°, ±15°,±30°, ±45°, ±60°, ±75°, 90°). The GA retrieval error indexes are plotted as functions of the spherical constraint coefficient (α) in Figure 8. As can be observed in this figure, the GA error index increases rapidly if the blending constraint (21) is not satisfied. These results demonstrate the potential loss of performance which can occur when retrieving stacking sequences while trying to match LPs obtained from an unconstrained continuous (i.e. no-blending constraints) optimisation. Results presented in Figure 8 also suggests that performance loss will remain low as long as the blending constraint is satisfied.

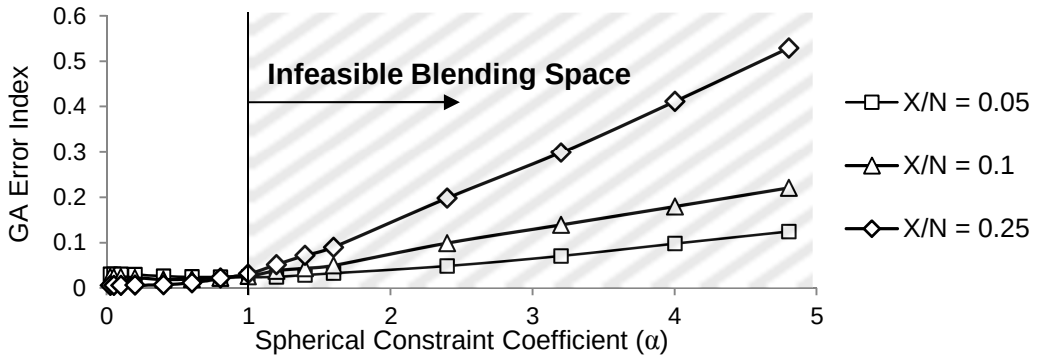

Figure 8 - Error index of the guide-based GA as a function of the spherical constraint coefficient α

3. Coupled In-plane Out-of-plane Lamination Parameters Blending Constraints

We have demonstrated, through the previous sections, that the change in lamination parameters due to ply-drops is limited. However, only in-plane lamination parameters were considered. In this Section, we propose a blending constraint which takes simultaneously into account all change in in-plane and out-of-plane lamination parameters. Since for most applications the coupling between in-plane and out-of-plane stiffness matrices is not desirable, only symmetric laminates are considered for the rest of this paper. Consequently, the number of ply-drops is restricted to positive integers multiple of 2 (i.e. N-2X) as shown in Figure 9.

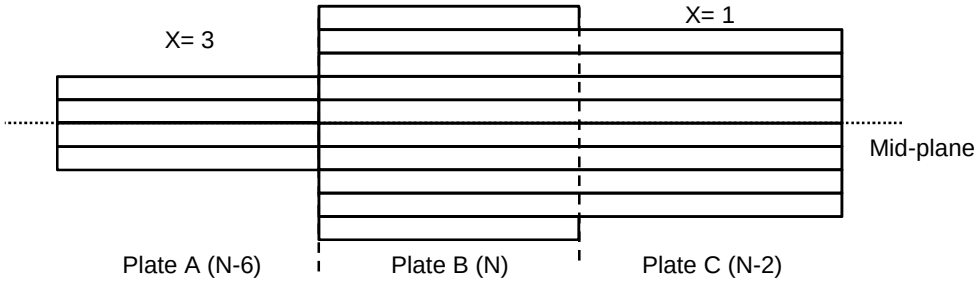

Figure 9 - Ply-drop illustration for symmetric laminates
(X is an integer, 2X is the number of ply-drops)

Similarly to Equation (10) for in-plane lamination parameters, it can be calculated that individual out-of-plane lamination parameters have to satisfy the following constraint:

$$\Delta V_k^D{}_{(N)\to(N-2X)} \leq \sqrt{f_k(\theta_j,\theta_i)}\ \ 2\left(3\left(\frac{X}{N}\right)-6\left(\frac{X}{N}\right)^2+4\left(\frac{X}{N}\right)^3\right), \qquad \text{for } k=1,2,3,4 \tag{22}$$

Note that the $f_k(\theta_j,\theta_i)$ function appears in both in-plane and out-of-plane constraints. Hence, one can easily combine constraints for in-plane and out-of-plane blending. The general hypersphere constraint is given:

$$\left(E_k^{ip,oop}{}_{(N)\to(N-X)}\right)^2 \leq f_k(\theta_j,\theta_i)\left[\underbrace{\left(\frac{2X}{N}\right)^2}_{In-Plane}+\underbrace{4\left(9\left(\frac{X}{N}\right)^2-36\left(\frac{X}{N}\right)^3+60\left(\frac{X}{N}\right)^4-48\left(\frac{X}{N}\right)^5+16\left(\frac{X}{N}\right)^6\right)}_{Out-of-Plane}\right] \tag{23}$$

Equation (23) is the final constraint derivation presented in this paper. It is a general equation which can be reduced to all previously presented results by simply substituting the $f_k(\theta_j,\theta_i)$ function values from Table 1. An application of the derived continuous blending constraints is now proposed.

IV. Application - Eighteen-panel Test Problem

In this section, the proposed continuous blending constraints are applied to a bi-step structural optimisation problem. The 18-panel horseshoe test problem [15] is used as a benchmark case study. Local loads, panel dimensions and material properties are fully known as shown in Figure 10. The panels thicknesses t_p and out-of-plane lamination parameters $V_1{}^D$ and $V_3{}^D$ are design variables (*dv*). The optimal design must minimise the structure weight (24) while satisfying the buckling load factor constraint (25) for each panel

$$\min f(dv) = \min \sum_{p=1}^{18} t_p \tag{24}$$

subject to,

$$1 - \lambda_p \leq 0\,, \quad \text{for} \quad p = [1,2,3,\ldots,18] \tag{25}$$

in which,

$$\lambda_p = \frac{\pi^2 \left[D_{11,p}\left(m/a_p\right)^4 + 2\left(D_{12,p} + 2D_{66,p}\right)\left(m/a_p\right)^2\left(n/b_p\right)^2 + D_{22,p}\left(n/b_p\right)^4 \right]}{N_{x,p}\left(m/a_p\right)^2 + N_{y,p}\left(n/b_p\right)^2} \tag{26}$$

where the subscript p denotes the panel number, $N_{x,p}$ and $N_{y,p}$ are the stress resultants in the longitudinal and transverse directions and $D_{ij,p}$ are the bending stiffness matrix terms of each panel. Parameters a_p and b_p denote the panel dimensions while m and n respectively refer to the number half wave length along the x and y directions. As for the original problem statement, the stiffness matrix terms D_{16} and D_{26} are assumed to be zero.

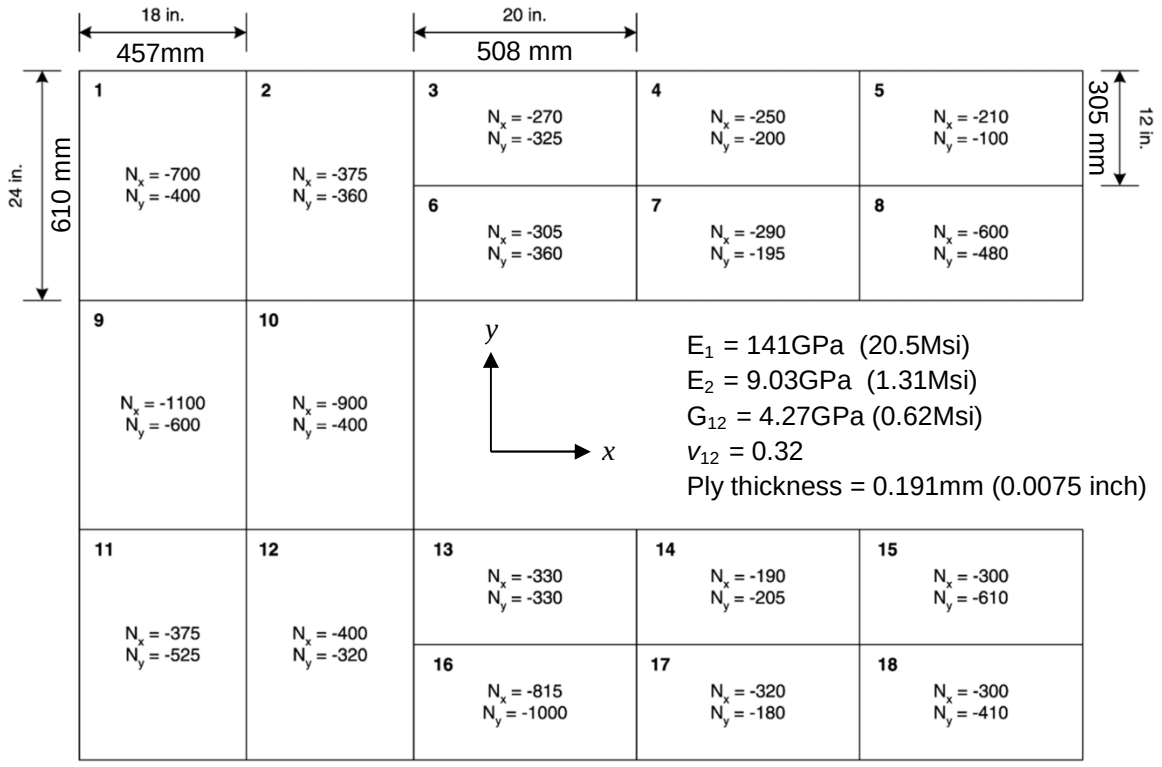

Figure 10 - Eighteen-panel blending test problem [15], N_x and N_y loads are in lbf/in (× 175.1 for N/m)

Selecting the blending constraints specific to the eighteen-panel test problem out of the general constraint formula (23), we have:

$$\left(\Delta V_k^D{}_{(Ni)\to(Nj)}\right)^2 \leq \alpha\, 4\left[4\left(9\left(\frac{X}{N}\right)^2 - 36\left(\frac{X}{N}\right)^3 + 60\left(\frac{X}{N}\right)^4 - 48\left(\frac{X}{N}\right)^5 + 16\left(\frac{X}{N}\right)^6\right)\right], \text{for } k = 1,3 \tag{27}$$

and

$$\left(\Delta V^{D}_{13_{(Ni)\to(Nj)}}\right)^2 \leq \beta\, 5.1443\left[4\left(9\left(\frac{X}{N}\right)^2 - 36\left(\frac{X}{N}\right)^3 + 60\left(\frac{X}{N}\right)^4 - 48\left(\frac{X}{N}\right)^5 + 16\left(\frac{X}{N}\right)^6\right)\right] \tag{28}$$

where *Ni* and *Nj* refer to two of the 18 panels, and the ply-drop or thickness ratio (X/N) between the panels is:

$$\frac{X_{\mathrm{ij}}}{N_{\mathrm{i}}} = \frac{N_{\mathrm{i}} - N_{\mathrm{j}}}{N_{\mathrm{i}}} = 1 - \frac{N_{\mathrm{j}}}{N_{\mathrm{i}}} = 1 - \frac{t_{\mathrm{j}}}{t_{\mathrm{i}}} \tag{29}$$

Note that in order to have a smooth analytical constraint, the continuous thicknesses are used to calculate the ply-drop ratio instead of the corresponding rounded values of the number of plies in Equation (29). As demonstrated in Section III, the maximal changes in LPs occur for extreme laminates. Since the default constraints (27) and (28) with $\alpha = \beta = 1$ are likely to be over-conservative, the variable coefficients α and β are introduced in order to investigate the impact of the constraints sphere radius on the optimisation results.

The proposed blending constraints (27) and (28) are spherical constraints which limit the change in LPs between laminates as a function of the laminates thickness ratio. However, enforcing these constraints when optimising both thicknesses and LPs simultaneously results in a non-convex optimisation problem. One algorithm, presented in in Figure 11, is proposed to solve this optimisation problem.

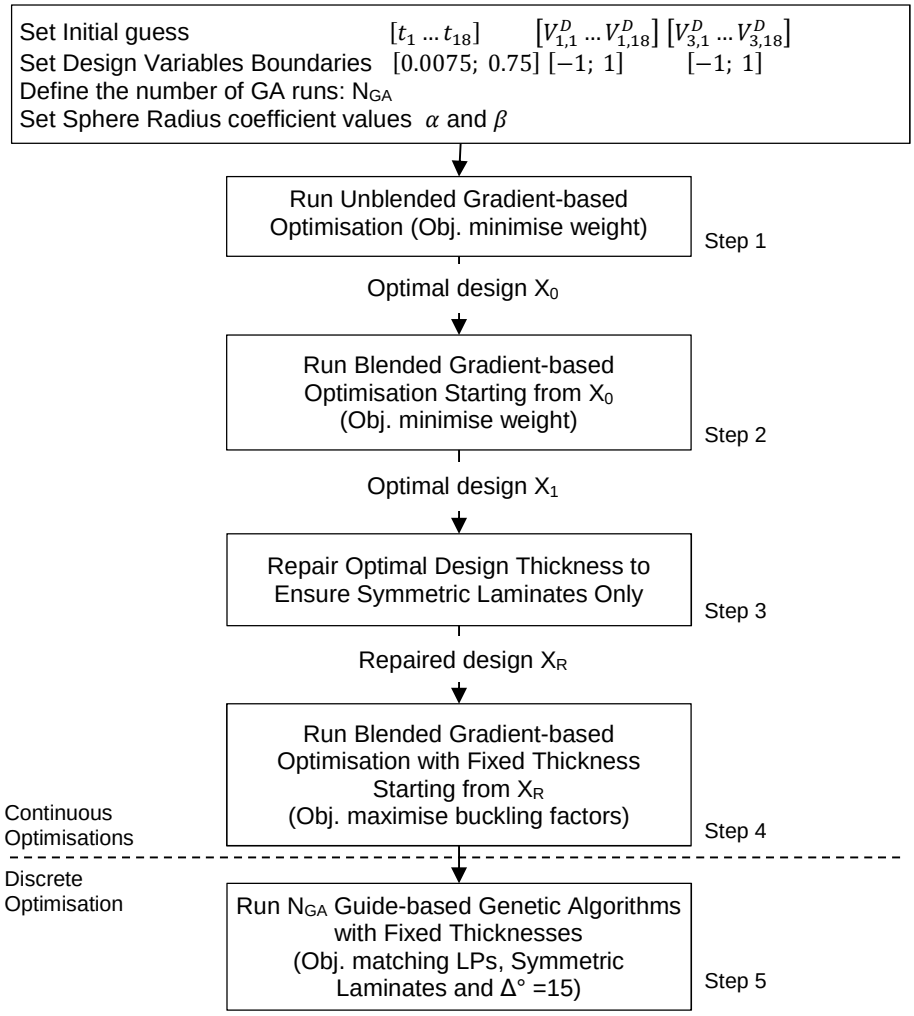

Figure 11 - Algorithm **1** for composite optimisation including blending constraints

Algorithm **1** first optimises the structure design (thicknesses and LPs) without blending constraints. In step 2, the unblended optimal design X_0 is used as the starting point of the blended optimisation (i.e. constraints (27) and (28) are active). The blended optimised design is stored in X_1. Up to this point, thicknesses remained continuous design variables during the optimisation. In step 3, a repair function rounds up the thicknesses of X_1 to an even number of plies. The repaired design (X_R) lamination parameters are optimised one last time while thicknesses are fixed (i.e. step 4). The propose 4 steps process from 1 to 4 is only one of the possible methods which can be used for integrating blending constraints into the continuous optimisation in order to achieve a more realistic continuous design. Investigating the impact of other approaches on the final continuous design is outside the scope of the present work.

Following the continuous optimisations, a guide-based GA is used to retrieve a blended stacking sequence. Since it is expected that the final continuous design (i.e. end of step 4) will be more realistic due to the application of blending constraints, it is likely that a close equivalent of this design can be found in the fibre angle space. In order to take advantage of this design equivalence and to avoid the computation of a potentially expensive fitness function, the guide-based GA objective is to match the LPs of the optimal continuous design.

MATLAB R2014b (*The MathWorks, Inc Natick, MA, USA*) was used to develop Algorithm **1**. The *fmincon* gradient-based optimisation tool provided by MATLAB was chosen to solve the smooth continuous optimisation problems. An in-house code has also been developed for the guide-based stacking sequence retrieval. Results obtained at each step of Algorithm **1** for a specific set of inputs are shown in Appendix A while the general results are presented in Figures 12,13 and 14. In these figures, the dashed line labelled 'Optimal Continuous Design (Step 1)' denotes the optimal results achieved at the end of step 1. This is the minimum weight design satisfying buckling constraints. On the other hand, the solid line 'Optimal (No Continuous Blending Constraints)' refers to the design obtained at the end of step 5 while skipping step 2 (i.e. no continuous blending constraint enforced). This solid line serves as a reference to evaluate the improvement achieved due to the application of our blending constraints. During results generation it was observed that because constraints (27) and (28) are coupled, the minimum spherical coefficients between α and β generally dominates the behaviour of the final results. For this reason, results are presented as a function of the minimal spherical radius coefficient.

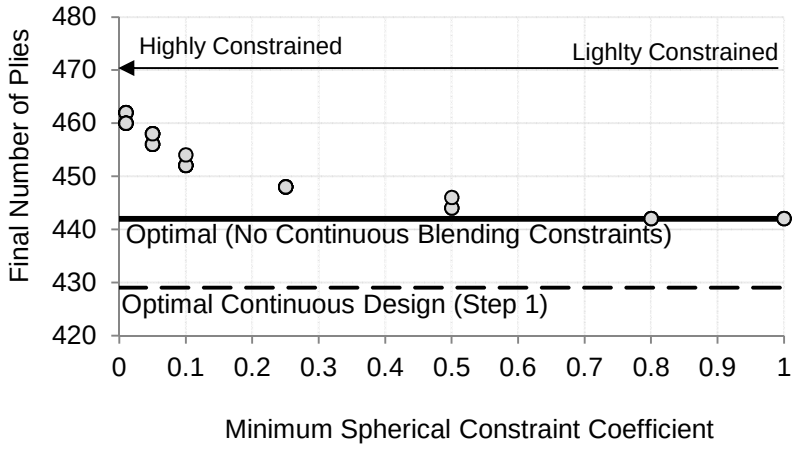

Figure 12 - Final number of plies obtained after optimisation (Step 5)

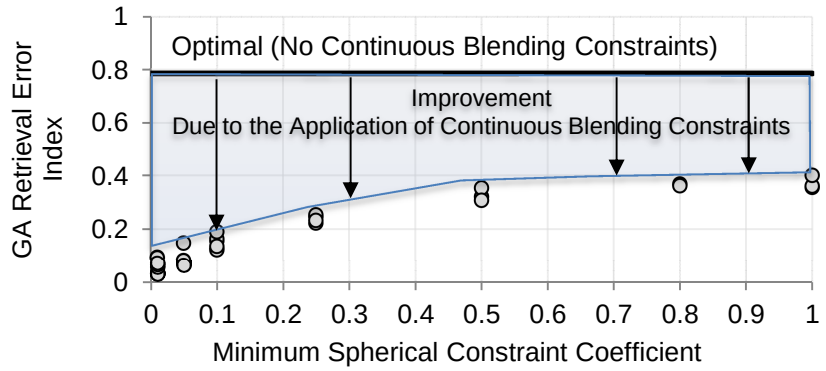

Figure 13 - GA retrieval error index (E_{index}). The lowest the value, the closer GA is matching the continuous LPs (Step 5)

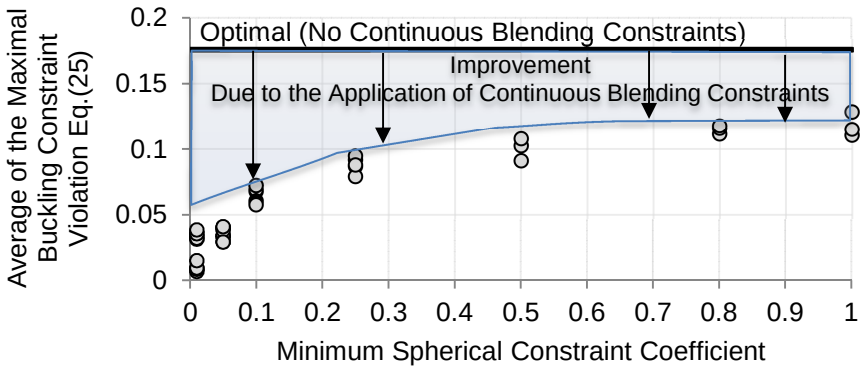

Figure 14 - Average of the maximal buckling constraint violation after GA (Step 5)

We first study the impact of the default constraints (i.e. $\alpha = \beta = 1$) on the optimisation results. As can be seen in Figure 12, the same number of plies is obtained with and without the application of the default value constraints (27) and (28). By contrast, it can be observed in Figures 13 and 14 that even the application of the default constraints results in a more realistic continuous design and a significant decrease in performance loss during stacking sequence retrieval. These results clearly highlight the benefit achieved by applying the proposed blending constraints during the continuous optimisation. Moreover, further improvement are observed when reducing the minimum spherical coefficients.

As shown in Figure 12, the number of plies of the optimal continuous design increases as the spherical constraint coefficients decrease. This result is to be expected since the minimal feasible weight (i.e. unblended optimal design) can only increase due to the addition of blending constraints. Likewise, a correlation between the capability of the GA to retrieve a matching stacking sequence (i.e. low error index) and the spherical constraint coefficients is observed in Figure 13. This observation confirms that constraining the change in LPs ease the retrieval of a stacking sequence for the benchmark test problem (i.e. generalisation of the results presented in Figure 8). To which extent the problem should be constrained in order to obtain a reasonable trade-off between the added number of plies and the continuous design increase feasibility remains, however, to be investigated.

Figure 14 presents the average (over 10 GAs) of the worst buckling factors obtained after stacking sequence retrieval. Similarly to Figure 13, the satisfaction of buckling constraints is seen to improve as the spherical constraints coefficient decreases. This is a direct consequence of the application of

blending constraints resulting in more realistic and easier-to-blend designs. However, note that while the optimal continuous design always satisfies buckling constraints, the retrieved stacking sequences never fully satisfy all constraints (i.e. positive constraint violation). This is explained as follows: at the end of step 4, the continuous optimisation reaches a design which is located on the boundary of the feasible continuous domain satisfying both blending and buckling constraints. The GA, by matching LPs instead of evaluating buckling factors, can only degrade or exactly match the continuous design performance. It is, therefore, necessary to introduce a safety factor (*SF*) for the proposed algorithms to achieve a final blended design satisfying all buckling constraints. This can be effortlessly implemented by modifying (25) as follows:

$$1(SF) - \lambda_p \leq 0\ , \quad \text{for} \quad p = [1,2,3,\dots,18] \tag{30}$$

A near optimal results achieved after stacking sequence retrieval employing this method is presented in Figure 15 and Table 2. Results are obtained after running Algorithm 1 with the inputs set to N_{GA} = 1, α=0.2, β=0.2 and a safety factor of 5 % ($SF = 1.05$). As can be seen in Figure 15, the optimal design LPs obtained at the end of the continuous optimisation (i.e. step 4) while enforcing blending constraints are located in the neighbourhood of single-step GA results reported in the literature [4, 6]. In addition to facilitate the retrieval of a blending stacking sequence, these results indicate that the application of continuous blending constraints for the horseshoe benchmark problem also effectively reduce the design search space around the global optimal. The retrieved stacking sequence is also closely located to the two previous results presented in literature.

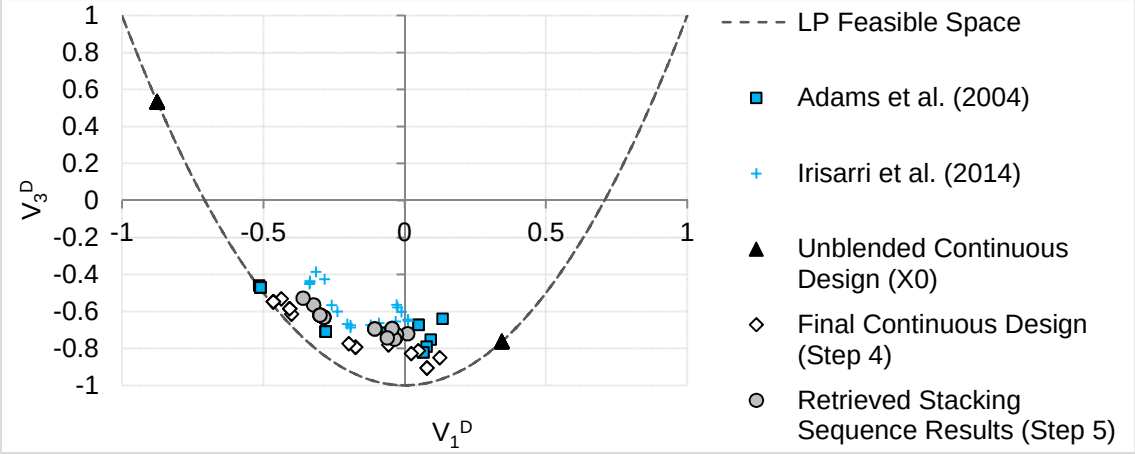

Figure 15 - Results comparison with the literature [4, 6]

Table 2 - Retrieved design example (the unsatisfied buckling factor constraints for n = m = 1 are shown in bold)

Panel	Nplies (460)	V_1^D	V_3^D	$(1-\lambda_p)$
1	34	-0.0296	-0.7379	-0.1128
2	28	-0.0442	-0.6930	**0.0172**
3	22	-0.2993	-0.6202	-0.2154
4	20	-0.2865	-0.6330	-0.3243
5	16	-0.3219	-0.5654	-0.1274
6	22	-0.2993	-0.6202	-0.0922
7	20	-0.2865	-0.6330	-0.2827
8	26	-0.1060	-0.6946	-0.1289
9	38	0.0105	-0.7203	-0.0071
10	36	-0.0284	-0.7262	-0.0840
11	30	-0.0360	-0.7504	-0.0557
12	28	-0.0442	-0.6930	**0.0214**
13	22	-0.2993	-0.6202	-0.1434
14	18	-0.3601	-0.5295	-0.0430
15	26	-0.1060	-0.6946	-0.0943
16	32	-0.0620	-0.7444	-0.1173
17	20	-0.2865	-0.6330	-0.3010
18	22	-0.2993	-0.6202	**0.0094**

V. Conclusion and Future Work

The present paper focuses on the application of blending constraints during the design of composite structures. Multi-step optimisation strategies employing a continuous and discrete optimisation step suffer from performance drops due to the design space discrepancy between the two optimisation steps. In general, the continuous optimisation is lightly or not constrained while the discrete optimisation is highly constrained. By deriving blending constraints applicable to continuous composite optimisation, the gap between the continuous and discrete optimisation levels can be reduced and the overall optimiser performance increased.

In the first part of this paper, the authors propose new blending constraints formulated in the lamination parameter space. Constraints for all coupling of in-plane and out-of-plane lamination parameters have been derived by quantifying the maximum change in lamination parameters resulting from ply-drops. Conservative spherical constraints based on these maximal values where subsequently proposed. It was observed that constraints for in-plane lamination parameters obey a simple linear relationship between the ply-drop ratio and the change in lamination parameters (see Equation (10)). Constraints for individual change in lamination parameters were also shown to be easily extendable to any combination of in-plane and out-of-plane lamination parameters (23).

In the second part of this investigation, the horseshoe blending test problem was used to provide an illustrative application of the newly derived blending constraints. The application of blending constraints was shown to result in more realistic optimal continuous designs for which the drop in performance between the two optimisation step was successfully reduced. However, to which extent the problem should be constrained in order to avoid excessive thickness increase remains unclear. In addition to the improve continuous design, the proposed implementation of blending constraint in Algorithm **1** has the advantage of reducing the genetic algorithm computational expense by replacing a potentially expensive fitness function by a fitness based on lamination parameter matching.

The present paper focused on the derivation of blending constraints. The applications of these constraints to other composite optimisation problems including the enforcement of additionally manufacturing constraints remains to be investigated. Furthermore, more in-depth studies are required in order to explain the choice of suitable spherical constraint coefficients resulting in a design space that is neither too restricted nor over-conservative.

Acknowledgment

Marco Tito Bordogna and Paul Lancelot have been supported in this work by funding from the People Programme (Marie Curie Actions) of the European Union's Seventh Framework Programme FP7 2012 under REA grant agreement n° 316394.

Appendix A. A Step by Step Example for Algorithm 1

The results obtained at each step of Algorithm **1** for a design case are presented herein. The options are set to: $N_{GA} = 10$, α=0.8, β=1.0 and no safety factor (SF=1). After generating a random initial design and running the unblended optimisation of step 1 we obtain:

Table 3 - Unblended (X_0) and blended (X_1) continuous design examples

	Unblended Continuous Design X_0				Blended Continuous Design X_1			
Panel	Nplies (429.09)	V_1^D	V_3^D	$(1-\lambda_p)$	Nplies (430.12)	V_1^D	V_3^D	$(1-\lambda_p)$
1	31.73	0.344	-0.763	-1.51E-09	31.73	0.318	-0.798	-2.54E-08
2	27.12	0.344	-0.763	-1.77E-09	27.12	0.307	-0.811	-3.23E-08
3	19.95	-0.876	0.534	-2.41E-09	19.95	-0.876	0.534	-3.85E-08
4	17.60	-0.876	0.534	-2.73E-09	17.60	-0.876	0.534	-4.36E-08
5	14.89	-0.876	0.534	-3.22E-09	14.89	-0.876	0.534	-5.16E-08
6	20.67	-0.876	0.534	-2.32E-09	20.67	-0.876	0.534	-3.72E-08
7	17.79	-0.876	0.534	-2.70E-09	17.79	-0.876	0.534	-4.32E-08
8	23.56	-0.876	0.534	-2.04E-09	23.60	-0.726	0.053	-3.08E-08
9	36.75	0.344	-0.763	-1.31E-09	36.75	0.344	-0.763	-2.09E-08
10	33.87	0.344	-0.763	-1.42E-09	33.87	0.344	-0.763	-2.27E-08
11	28.50	0.344	-0.763	-1.68E-09	28.58	0.186	-0.931	-1.82E-08
12	27.16	0.344	-0.763	-1.77E-09	27.16	0.315	-0.802	-2.94E-08
13	20.36	-0.876	0.534	-2.36E-09	20.36	-0.876	0.534	-3.77E-08
14	17.26	-0.876	0.534	-2.78E-09	17.26	-0.876	0.534	-4.45E-08
15	23.81	-0.876	0.534	-2.02E-09	23.87	-0.697	-0.029	-2.86E-08
16	28.97	-0.876	0.534	-1.66E-09	29.88	-0.239	-0.886	-4.35E-08
17	17.70	-0.876	0.534	-2.71E-09	17.70	-0.876	0.534	-4.34E-08
18	21.35	-0.876	0.534	-2.25E-09	21.35	-0.876	0.534	-3.60E-08

Table 4 - Final Continuous and retrieved design examples

Panel	Nplies (442)	Final Continuous Design (Step 4)			GA Retrieved Design (Step 5)		
		V_1^D	V_3^D	$(1-\lambda_p)$	V_1^D	V_3^D	$(1-\lambda_p)$
1	32	0.208	-0.843	-0.0064	-0.163	-0.679	0.1164
2	28	0.092	-0.714	-0.0235	-0.199	-0.636	0.0700
3	20	-0.722	0.054	-0.0015	-0.546	0.000	0.0601
4	18	-0.582	-0.228	-0.0385	-0.451	-0.224	0.0151
5	16	-0.477	-0.235	-0.1564	-0.442	-0.224	-0.1382
6	22	-0.469	-0.335	-0.1326	-0.410	-0.249	-0.0945
7	18	-0.582	-0.228	-0.0059	-0.451	-0.224	0.0460
8	24	-0.597	-0.252	-0.0346	-0.316	-0.421	0.0590
9	38	0.192	-0.657	-0.0438	0.056	-0.654	-0.0065
10	34	0.308	-0.776	-0.0053	-0.088	-0.685	0.1091
11	30	-0.241	-0.816	-0.0108	-0.162	-0.704	-0.0102
12	28	0.092	-0.714	-0.0191	-0.199	-0.636	0.0740
13	22	-0.469	-0.335	-0.1856	-0.410	-0.249	-0.1457
14	18	-0.582	-0.228	-0.1015	-0.451	-0.224	-0.0447
15	24	-0.597	-0.252	-0.0029	-0.316	-0.421	0.0878
16	30	-0.241	-0.816	-0.0050	-0.162	-0.704	0.0421
17	18	-0.582	-0.228	-0.0202	-0.451	-0.224	0.0324
18	22	-0.469	-0.335	-0.0272	-0.410	-0.249	0.0074

The lamination parameters obtained at the various step of the optimisation are illustrated in Figure 16.

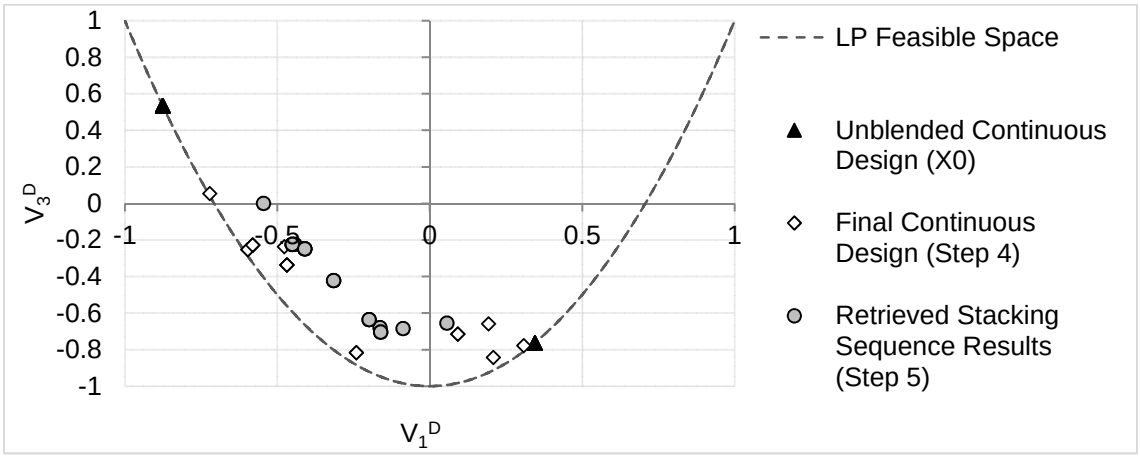

Figure 16 - Lamination parameters obtained at steps 1,4 and 5 of Algorithm **1**

VI. References

[1] Ghiasi H, Fayazbakhsh K, Pasini D, Lessard L. Optimum stacking sequence design of composite materials Part II: Variable stiffness design. Composite Structures. 2010;93:1-13.

[2] Ghiasi H, Pasini D, Lessard L. Optimum stacking sequence design of composite materials Part I: Constant stiffness design. Composite Structures. 2009;90.

[3] Vincenti A, Vannucci P, Ahmadian MR. Optimization of laminated composites by using genetic algorithm and the polar description of plane anisotropy. Mechanics of Advanced Materials and Structures. 2013;20:242-55.

[4] Irisarri F-X, Lasseigne A, Leroy F-H, Le Riche R. Optimal design of laminated composite structures with ply drops using stacking sequence tables. Composite Structures. 2014;107:559-69.

[5] Kristinsdottir BP, Zabinsky ZB, Tuttle ME, Neogi S. Optimal design of large composite panels with varying loads. Composite Structures. 2001;51:93-102.

[6] Adams DB, Watson LT, Gürdal Z, Anderson-Cook CM. Genetic algorithm optimization and blending of composite laminates by locally reducing laminate thickness. Advances in Engineering Software. 2004;35:35-43.
[7] Peeters DM, Hesse S, Abdalla MM. Stacking sequence optimisation of variable stiffness laminates with manufacturing constraints. Composite Structures. 2015;125:596-604.
[8] Dillinger J, Klimmek T, Abdalla M, Gürdal Z. Stiffness optimization of composite wings with aeroelastic constraints. Journal of aircraft. 2013;50:1159-68.
[9] Liu D, Toroporov VV, Querin OM, Barton DC. Bilevel optimization of blended composite wing panels. Journal of aircraft. 2011;48:107-18.
[10] IJsselmuiden ST, Abdalla MM, Seresta O, Gürdal Z. Multi-step blended stacking sequence design of panel assemblies with buckling constraints. Composites Part B: Engineering. 2009;40:329-36.
[11] Liu S, Hou Y, Sun X, Zhang Y. A two-step optimization scheme for maximum stiffness design of laminated plates based on lamination parameters. Composite Structures. 2012;94:3529-37.
[12] Van Campen J, Gürdal Z. Retrieving variable stiffness laminates from lamination parameters distribution. Proceedings of the 50th AIAA/ASME/ASCE/AHS/ASC structures, structural dynamics and materials conference, Palm Springs, CA2009.
[13] Van Campen J, Seresta O, Abdalla MM, Gürdal Z. General blending definitions for stacking sequence design of composite laminate structure. Proceedings of 49th AIAA/ASME/ASCE/AHS/ASC structures, structural dynamics, and materials conference, Schaumburg, IL, USA2008. p. 7-10.
[14] Liu B, Haftka RT. Composite wing structural design optimization with continuity constraints. Proceedings of 42nd AIAA/ASME/ASCE/AHS/ASC Structures, Structural Dynamics, and Materials Conference, AIAA Paper2001.
[15] Soremekun G, Gürdal Z, Kassapoglou C, Toni D. Stacking sequence blending of multiple composite laminates using genetic algorithms. Composite Structures. 2002;56:53-62.